IOSR Journal of Applied Chemistry (IOSR-JAC)
e-ISSN: 2278-5736. Volume 18, Issue 3 Ser. 1 (March 2025), PP 61-70
www.iosrjournals.org

Sulphate Modified Cu-Co Bimetallic MOF as a Potential Catalyst for Glycerol Acetalization to Solketal

Vennela Aluvala[1], Balakrishna Matkala[1], Venkatesham Kothabai[1], Vijayalaxmi Burri[1], Sasikumar Boggala[2], Anjaneyulu Chatla[2], Sreedhar Inkollu[3], Hari Padmasri Aytam[1*]

[1] *Department of Chemistry, University College of Science, Osmania University, Hyderabad 500 007, Telangana, India*

[2] *Catalysis and Fine Chemicals Department, CSIR - Indian Institute of Chemical Technology, Hyderabad-500 007, Telangana, India.*

[3]*Department of Chemical Engineering, Birla Institute of Technology and Science, Pilani, Hyderabad 500 078, Telangana, India.*

**For Correspondence: ahpadmasri@osmania.ac.in; ahpadmasri@gmail.com*

Abstract

Sulphate modified bimetallic Cu-Co MOF was explored for the valorization of glycerol to solketal at ambient conditions. Co MOF on modification by incorporating Cu to synthesize bimetallic Cu-Co MOF proved to be advantageous in exhibiting enhanced activity towards the formation of solketal due to the increase in Lewis acid sites on the surface of the catalyst. Sulphated Cu-Co MOF was synthesized by solvo-thermal method followed by impregnation and the thus synthesized catalyst was well characterized by XRD, N_2 sorption to measure BET-SA, SEM-EDS, FT-IR, Raman, Ex-situ Py-adsorbed IR spectroscopy to correlate the physico-chemical characteristics of the catalyst studied with its activity. The activity of sulphated Cu-Co MOF was compared with its parent Cu-Co MOF form and the monometallic Co-MOF both in parent and sulphated forms. The activity of sulphated Cu-Co MOF was much higher as compared to the rest three of the catalysts which matched with the order of their acidities especially the no. of Lewis acid sites as confirmed from the Ex-situ Py-IR studies. The sulphated bimetallic MOF exhibited stable activity even after 5 times of reuse and the used catalyst XRD, SEM-EDS and CHNS analyses indicated the structure to be intact and without loss of sulphate . Sulphate modified Cu-Co MOF was shown to be a potential catalyst for the valorization of glycerol to solketal.

Key Words: *Cu-Co MOF; glycerol; acetalization; sulphation; Lewis acid sites; Py-IR*

Date of submission: 14-03-2025 Date of acceptance: 27-03-2025

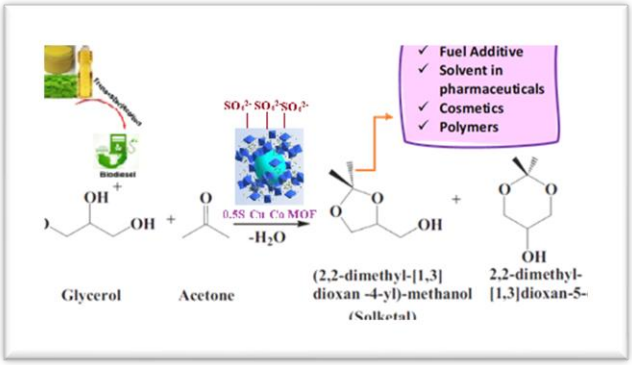

Scheme 1: Glycerol Acetalization over sulphated Cu-Co MOF

I. Introduction

Metal Organic Frameworks (MOFs) are a special class composed of metal nodes and organic linkers making up a tunable structure of different dimensionality, high surface area, microporosity and micro crystallinity [1,2]. These characteristic features are responsible for the wide range applications of these materials in gas separations, optical devices, biomimicking, photocatalysis, gas sensors and adsorption of various organic molecules and removal of pollutants[3-7]. With the presence of higher number of active sites attributed to their

versatile nature of forming high specific surface area structures, well-defined pores with different range of metal ions and organic ligands, MOFs can be harvested for heterogeneous catalytic reactions. MOFs are being extensively studied for various oxidation, hydrogenation, dehydrogenation, C-H activation and coupling reactions [8-12]. Central metal ions were suggested as the active sites for adsorption in the study of various MOFs as adsorbents and catalysts. Bimetallic MOFs were thus opined to be advantageous in generating these active sites that enhance the capabilities of MOFs as adsorbents and catalysts [13]. In the present work Cu-Co bimetallic MOF is chosen with available information that Co can easily be substituted with Cu possessing similar ionic radii generating alike crystalline structure and similar coordinatively unsaturated sites (metal ion sites) that active in catalyzing various heterogeneous reactions [14].

Glycerol is a by-product obtained in good amounts in the production of bio-diesel by transesterification reaction [15-17]. This process produces about 10-15% of glycerol which accounts for large amounts that can reduce the economic viability of bio-diesel production. Bio-diesel is one of the alternative fuels produced from a renewable resource to fill up the gaps created by reduced production of fuels from non-renewable resources. Glycerol is also a platform chemical that can a feed stock to synthesize variety of other chemicals through different organic transformations[18-21]. Acetalization of glycerol to solketal, a fuel additive, a less toxic and a value-added compound due to its application as solvent in ink and paint industry, as a component in pharmaceuticals, polymers, cosmetics and drug delivery materials, is an efficient means of utilization of glycerol[22-25]. Glycerol reaction with acetone to form solketal is an acid-catalyzed reaction. It is well documented for the efficient synthesis of solketal over zeolite-based catalysts, heteropoly acids, modified carbonaceous materials, metal oxides, modified mesoporous silica catalysts[26-35]. A few reports are also available recently on the use of MOFs for the solketal synthesis by acetalization of glycerol[36-38].

The present work is the exploration of the advantageous properties of sulphated bimetallic Cu-Co MOF material as a potential catalyst for the effective valorization of glycerol to solketal. The synthesis of Cu-Co MOF and its modification by sulphation of the MOF, characterization of the synthesized MOF by various adsorption and spectroscopic techniques to understand the physico-chemical characteristic features of Cu-Co MOF and its use in the glycerol conversion to solketal was discussed in this report.

II. Experimental methods

Chemicals Used

Copper nitrate, Cobalt nitrate, 1,3,5-benzene tricarboxylic acid (BTC), DMF, Ethanol, Acetone, Glycerol were of Sigma-Aldrich and Spectrochem Make, AR grade. All the chemicals were used as such without any further treatment.

Preparation of Cu-Co MOF & Sulphated Cu-Co MOF

Cu-Co BTC MOF is prepared using solvo-thermal technique by the mixing of two metal nitrate solutions (with Cu/Co atomic ratio = 0.6) dissolved in 1:1 ratio of DMF and ethanol mixture. This mixture after thorough mixing was autoclaved for hydrothermal treatment at 85 °C for 24 h. Then the mother liquor thus obtained was decanted and washed thoroughly with DMF and ethanol. The solid got from after the washings was dried at 170 °C in a vacuum oven for 6 h to get Cu-Co BTC MOF.

1g of Cu-Co MOF is taken and impregnated with 0.5 N sulphuric acid solution, stirred slowly for 2h at 25 ºC, washed thoroughly with deionized water and dried in an oven for overnight at 100 ºC. The resultant material was labelled as 0.5S-Cu-Co MOF.

Co BTC MOF was prepared similar to the procedure mentioned above for Cu-Co BTC MOF for comparing the activity of the bimetallic MOF with that of the monometallic MOF catalysts. The sulphated monometallic MOF was also synthesized as the sulphated Cu-Co MOF and labelled as 0.5S-Co MOF.

Characterization of Catalysts

The bimetallic and monometallic MOFs and their sulphated MOFs were all subjected to different adsorption and spectroscopic techniques to characterize their physico-chemical properties in understanding their catalytic performance towards glycerol acetalization reaction. The X-ray diffractograms were recorded on a Rigaku Miniplex diffractometer using CuK_{α} radiation. BET-surface area was calculated by N_2 sorption isotherms obtained at liquid nitrogen temperature on a Micromeritic ASAP 2010 surface area analyzer. FT-IR spectra and the Ex-situ pyridine adsorbed IR spectra (after an exposure of pyridine vapours for 2h) of the samples were recorded on a Varian 660-IR spectrometer. A JEOL JSM-6010/LA microscope was used to scan the samples for the SEM micrographs and EDS spectra. Raman spectra were recorded using HORIBA JOBIN YVON HR800, Japan spectrometer using a He-Ne LASER of wavelength 633 nm.

Experimental details of Activity evaluation

Glycerol-Acetone reaction was carried out in a glass made batch reactor with reaction mixture subjected to continuous stirring in presence of a catalyst over a magnetic stirrer. The reaction parameters namely reactants mole ratio, catalyst amount, time on stream studies and recyclability of the catalyst were studied and the products were analyzed at a definite time period using an Agilent 1020A GC provided with FID detector and confirmed

by GC-MS. The catalyst was removed by centrifugation from the product mixture, washed thoroughly by acetone and water, dried in oven before reuse in the reaction. The following equations are used for calculating the conversion of glycerol, selectivity of solketal and rate of formation of solketal:

$$Conversion\ (\%) = \frac{No.of\ initial\ moles\ of\ glycerol - No.of\ final\ moles\ of\ glycerol}{No.of\ initial\ moles\ of\ glycerol}$$

$$Selectivity\ of\ Solketal\ (\%) = \frac{moles\ of\ Solketal\ formed}{Moles\ of\ glycerol\ converted} \times 100$$

$$\text{Rate}_{\text{Solketal}} = \frac{Yield\ of\ solketal \times moles\ of\ glycerol\ feed}{amount\ of\ catalyst(g) \times time(h)}$$

III. Results and Discussion

X-ray diffraction analysis

The MOF phase formation of Cu-Co bimetallic MOF was confirmed from the X-ray diffractograms shown in figure 1. The presence of peaks at 2theta = 6.6°, 9.44°, 11.76°, 13.71°, 15.14°, 16.73°, 17.16°, 19.23°, 25.92°, and 28.92° correspond to the planes (2 0 0), (2 2 0), (2 2 2), (4 0 0), (3 3 1), (4 2 2), (5 5 1), (4 4 0), (7 3 1) and (7 51) respectively which indicate the Cu-BTC MOF phase (JCPDS no. 00-062-1183) without any other phases showing the absence of impurities [39]. The diffraction peaks that were observed at 17.50°, 17.78°, 18.68°, 20.01°, 21.29°, and 21.92° represent (220), (310), (111), (021), (201), and (400) crystal planes of Co–BTC MOF [40]. The average crystallite size of the bimetallic MOF sample obtained from Scherrer formula is 11.6 nm which is slightly larger than its corresponding monometallic MOFs viz., Co MOF catalyst. The XRD patterns of the sulphated MOFs show no structural changes upon sulphation indicating an intact MOF structure. However, a slight broadening of peaks resulting in the reduced crystallite size of sulphated samples could be observed in the patterns of their XRD.

Table 1: Physico-Chemical characteristics of Cu-Co MOFs

Catalysts	BET-SA (m^2g^{-1})	Crystallite Size (nm) from XRD	$I_{Lewis}/I_{Bronsted}$ from Ex-situ Py-IR
Cu-Co MOF	863	11.6	0.58
Co MOF	802	6.3	0.41
0.5S-Cu-Co MOF	734	7.1	1.13
0.5S-Co MOF	656	5.2	0.67

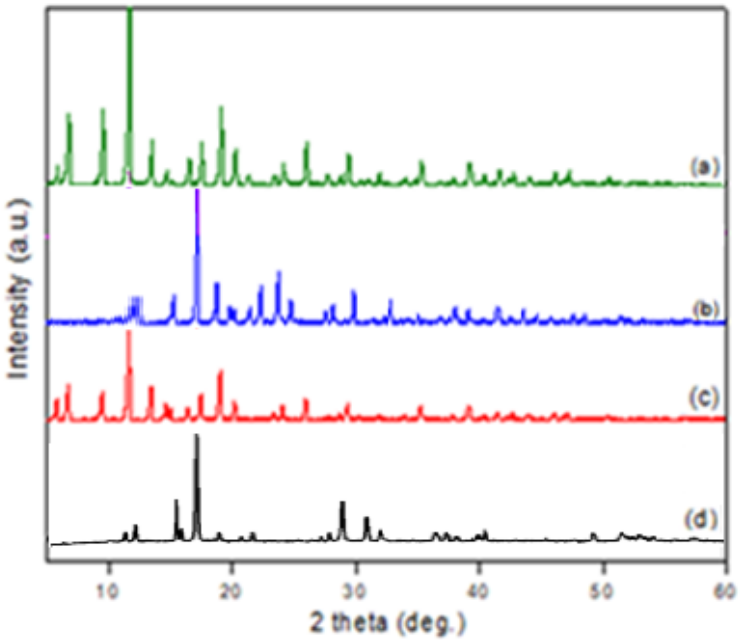

Figure 1: X-ray diffractograms of (a) Cu-Co (b) Co (c) sulphated Cu-Co (d) sulphated Co MOFs

N_2 Sorption results

The adsorption isotherms indicated the microporous nature of the MOFs from the type I isotherms seen (not shown here) and the calculated BET-surface area values are quite high presented in table 1 confirming the high specific surface area characteristic of MOF materials. The surface area of bimetallic MOF was in between that of Cu-MOF and Co-MOF with Co-MOF displaying slightly higher specific surface than the bimetallic and Cu-MOF catalysts. The pore size values also indicate the microporous nature of the MOFs synthesized.

Morphological studies

SEM images indicate a polyhedron (cubo and cubo octahedron) morphology of the bimetallic MOF sample. An average particle size of ~ nm was indicated from the micrograph (figure 2a). The EDS spectra and elemental mapping (figure 2b & 3) clearly establish the presence of various elements viz., Cu, Co, O and C in the synthesized Cu-Co MOF. Sulphated bimetallic Cu-Co MOF sample also showed similar morphology in the SEM analysis and an additional element S was shown in the EDX spectra of the sample (figures not shown here).

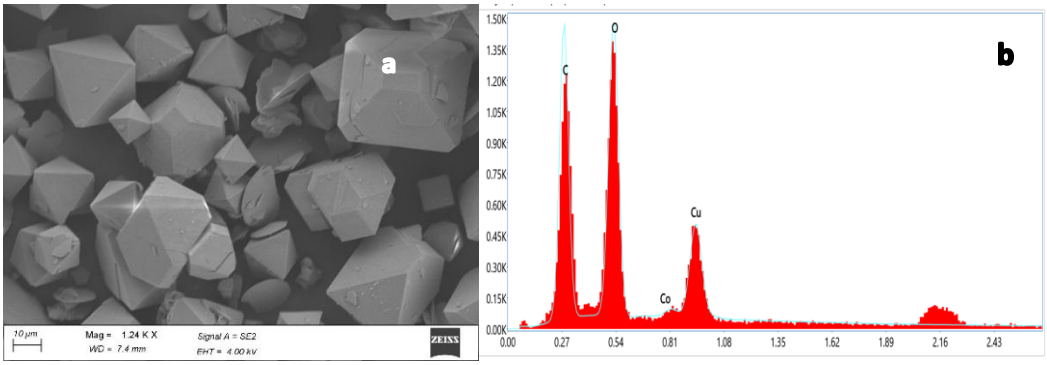

Figure 2. SEM-EDS images of Cu-Co MOF

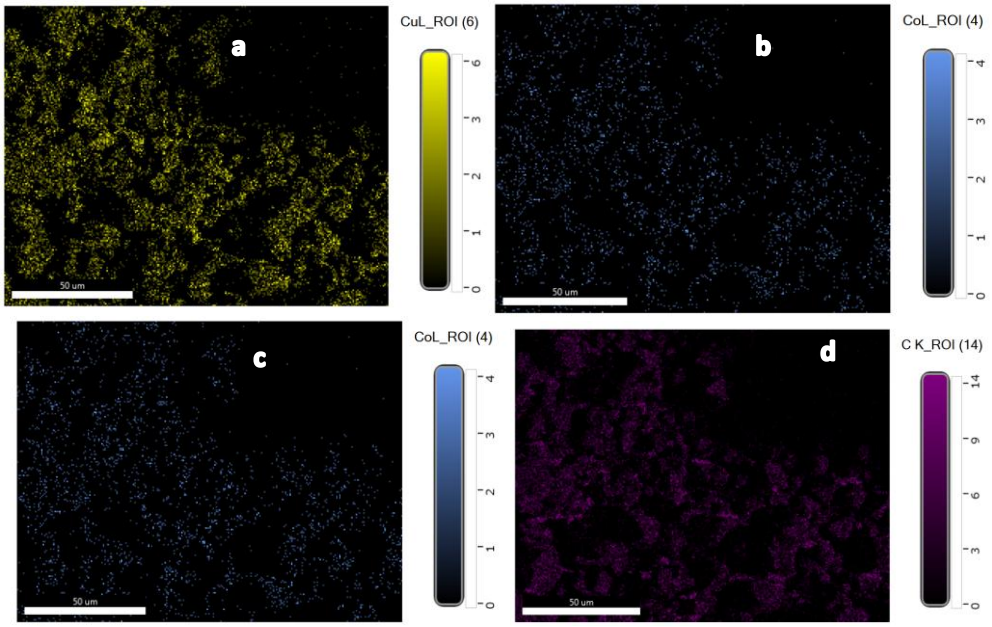

Figure 3. EDS elemental mapping of a) Cu b) Co (c) O and (d) C of Cu-Co MOF

FT-IR Spectral data

FT-IR spectra displayed below as figure 4 indicates the typical symmetric and asymmetric stretching modes of the organic linker BTC in the range of 1628-1370 cm^{-1}. The band in between 1628-1565 cm^{-1} corresponding to asymmetric vibrational mode while that in between 1445-1370 cm^{-1} is caused by symmetric stretching exhibited by the carbonyl group of BTC. The deprotonation of BTC is responsible for the absence of any peak around 1726-1680 cm^{-1} that is usually seen in case of carboxylic acid groups. Other peaks at ~1102 and 715 cm^{-1} can be assigned to the vibrational stretching frequencies of C–H bond and Cu^{2+} coordinated to the carboxylate ions of BTC respectively [41]. The bands in between 400-600 cm^{-1} correspond to Cu-O and Co-O interactions [42]. The sulphated MOFs have shown (figure 5) some additional peaks at 580 and 883 cm^{-1} and, 1288 cm^{-1} corresponding to symmetric and asymmetric vibrations of sulphate group (S=O) respectively [43, 44]. However, the cluster of peaks of BTC are very close to that of the sulphate vibrational modes that could not be

clearly distinguished in the spectra. But, the S=O peak was quite broad and shifted towards lower frequency in sulphated Cu-Co MOF as compared to that on sulphated Co-MOF. It seems greater sulphate group seem to bind due to the availability of two types of metal ions that are present in the structure.

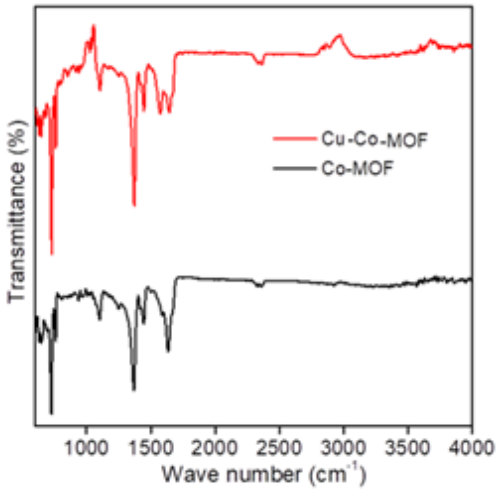

Figure 4. FT-IR of Cu-Co MOF & Co-MOF

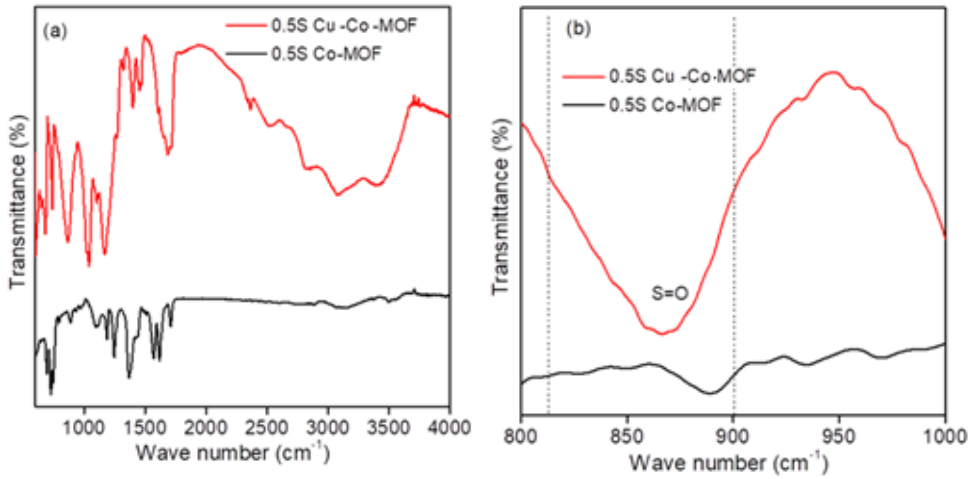

Figure 5. FT-IR of sulphated Cu-Co MOF & Co MOF

Raman Spectral Analysis

The characteristic Raman bands were obtained in between 200-270 cm^{-1} and a weak peak ~470 cm^{-1} which can be ascribed to Cu-Cu and Cu-O stretching vibrations respectively in figure 6 represented from the Raman spectral data obtained for the sulphated Cu-Co and Co MOFs. The signals at 1494 cm^{-1}, 1609 cm^{-1} (not shown in the figure) and at 864 and 895 cm^{-1} correspond to the O–C=O, C–H and C=C groups of the BTC organic linker [45, 46]. The peaks in the range of 250–630 cm^{-1} are suggested as the vibrational modes of Co^{2+} linked to the O of carboxylate group of BTC [47].

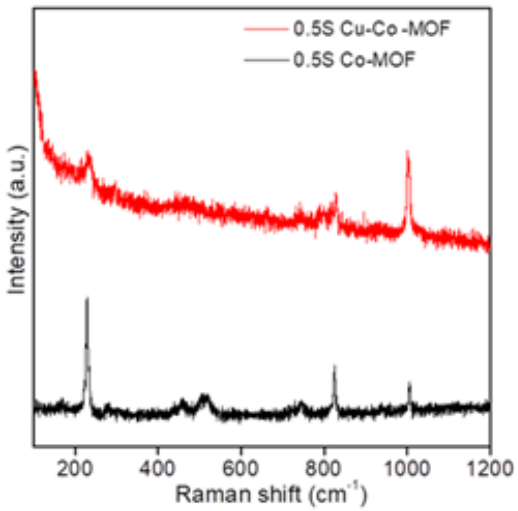

Figure 6. Raman spectra of sulphated Cu-Co MOF & Co MOF

Ex-Situ Py-IR Analysis

Solketal is formed from glycerol by acetalization reaction which is an acid catalyzed reaction. Acidity of the catalyst and type of acid sites govern the selectivity and yields of solketal formation. The literature reports indicate that greater no. of acid sites available on the surface of the catalysts can give higher yields of this product. Certain reports [48, 49] suggest the Bronsted acid sites playing dominant role in the selective formation of solketal while others report Lewis acid sites being the key sites in determining the solketal formation rate [28, 50]. The type of acid sites and their strengths were measured by Ex-situ Py-adsorbed FT-IR spectra in this study. The figure 7 below indicates that there is a significant enhancement in acidity of both monometallic Co-MOF as well as bimetallic Cu-Co MOF catalysts with sulphonation depicted by the increase in the intensity of peaks at ~1560 cm^{-1} and ~1450 cm^{-1} which are ascribed to the pyridine linkage to Bronsted acid sites and Lewis acid sites respectively. However, it is also evident that there is a greater increase in the Lewis acid sites as against the enhancement in Bronsted sites seen in these spectra and indicated as the higher $I_{Lewis}/I_{Bronsted}$ ratio presented in table 1. This probably signifies the synergistic role played by the well substituted Cu ions in the Co-MOF structure forming the bimetallic Cu-Co MOF and greater availability of these metal ions for the catalytic process.

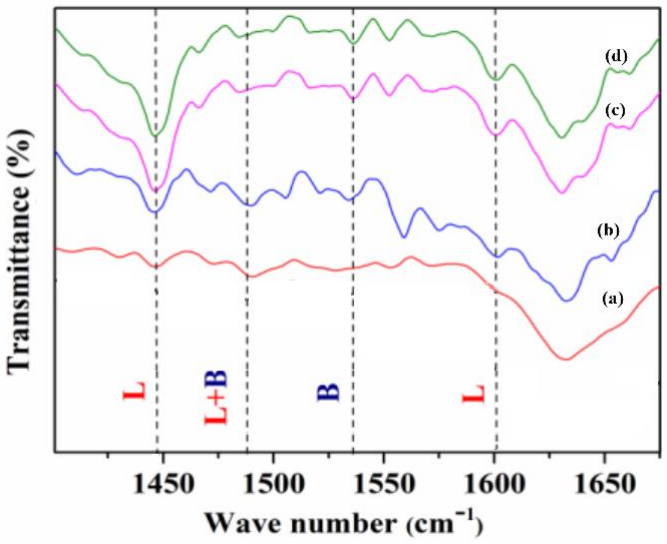

Figure 7. Ex-situ Py-IR spectra of (a) Co-MOF (b) Cu-Co MOF (c) 0.5S-Co MOF (d) 0.5S-Cu-Co MOF catalysts

Activity Studies

Acetalization of glycerol with acetone was studied under variable conditions of reactants mole ratio, time on stream and catalyst amounts over Cu-Co MOF catalyst. The activity of this bimetallic catalyst was compared to the monometallic Co-MOF catalysts. Initially the reaction was aimed over Co-MOF catalyst for the

acetalization of glycerol to solketal. However, the conversion was observed to be poor over this catalyst though some improvement could be seen with sulphation of the catalyst, the conversion of glycerol was still low as can be seen in figure 8. The incorporation of Cu has dramatically raised the conversion of glycerol and selectivity towards solketal formation. This clearly demonstrated the advantageous role played by the bimetallic MOF in the effective transformation of glycerol to solketal. Figure 8 below displays the glycerol acetalization at ambient conditions and optimized reaction conditions of 1:10 mole ratio of glycerol : acetone, 180 min. of steady-state conversion and 4wt.% of catalyst used in the study. A comparative activity of glycerol and acetone reaction to form solketal over parent Co-MOF, Cu-Co MOF, sulphated Co-MOF and sulphated Cu-Co MOF is presented in this figure which demonstrates the higher conversion of glycerol and selectivity of formation towards solketal over the sulphated bimetallic Cu-Co MOF catalyst. The reason behind this could be explained from the ex-situ Py-IR studies that indicated the presence of higher no. of Lewis acid sites over this catalyst as compared to rest of the catalysts studied. The synergistic influence of Cu^{2+} whose ionic radii is a close match to that of Co^{2+} could be witnessed with the drastic increase in the conversion levels of glycerol observed when Cu was added into Co-MOF system. Addition of Cu ion species probably increase the sulphate binding sites that enhanced the surface available Lewis acid sites for glycerol chemisorption which in turn increased the rate of solketal formation.

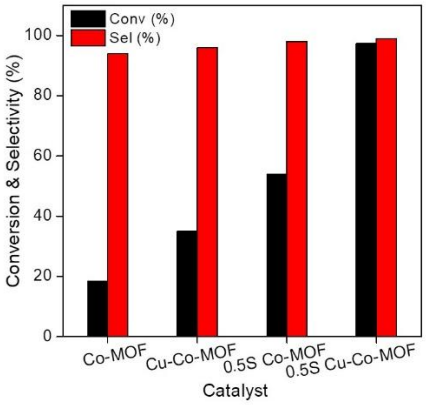

Figure 8. Glycerol acetalization activity over MOF catalysts

Bimetallic Cu-Co MOF was subjected to the optimization of reaction parameters by varying the reactants mole ratios from 1:4-1:10, catalyst amounts ranging from 1wt.% to 5wt.% and reaction time up to 180 min. The data from these studies is presented in figure 9 A, B and C. It can be concluded from the figures that a mole ratio of 1:10 of glycerol : acetone, 4wt.% of catalyst and 180 min. of time on stream are optimum in producing solketal in higher yields. Thus, these conditions were chosen in the comparative study of the sulphated bimetallic Cu-Co MOF with those of the other three catalysts studied (figure 8).

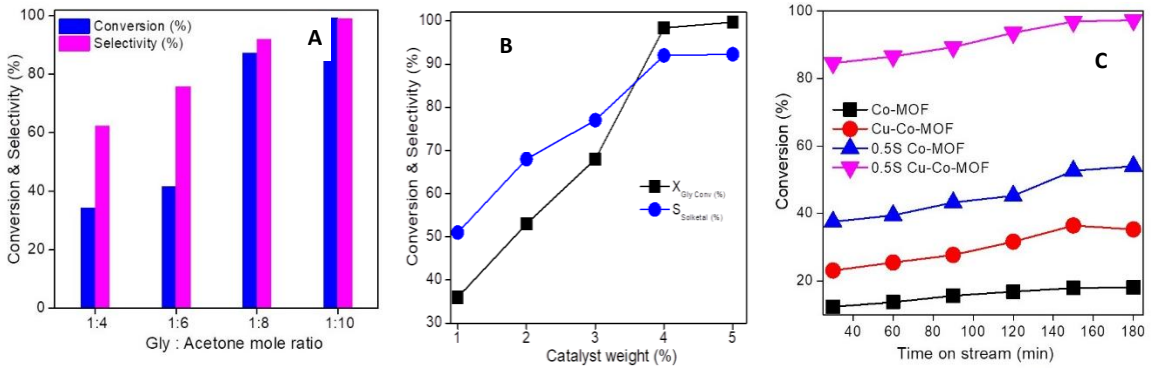

Figure 9. Effect of A) Glycerol : Acetone mole ratio B) Catalyst amount glycerol acetalization over 0.5S-Cu-Co MOF and C) Time on stream activity of MOF catalysts

Reusability studies

The catalyst was found to be stable enough without much loss in activity even after 5 cycles of use in the glycerol acetalization reaction over 0.5S-Cu-Co MOF. The catalyst was centrifuged, filtered, washed with acetone and then water before drying it in oven after every reaction run. This was then used for the reaction in the next cycle. The figure 10 below shows the stable activity of the catalysts for 5 cycles of use. The catalyst used for 5 cycles was tested by XRD and SEM analyses to confirm the stability of the catalyst. The figures 11 A & B clearly

establish the structure being intact. EDX(data not shown here) and CHNS analyses data presented in table 2 of the used sulphated bimetallic catalyst further indicate no loss of any sulphate, retaining the acidity of the catalyst that may be attributed to its stable activity.

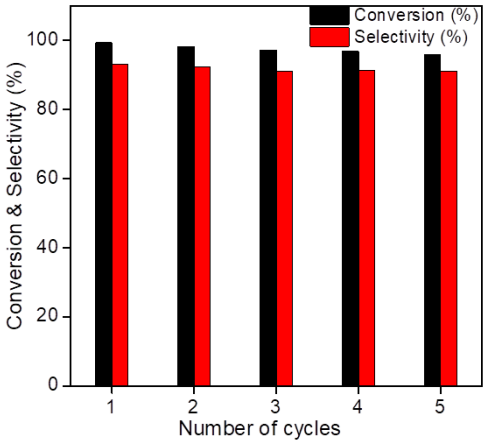

Figure 10. Reusability of 0.5S-Cu-Co MOF catalyst

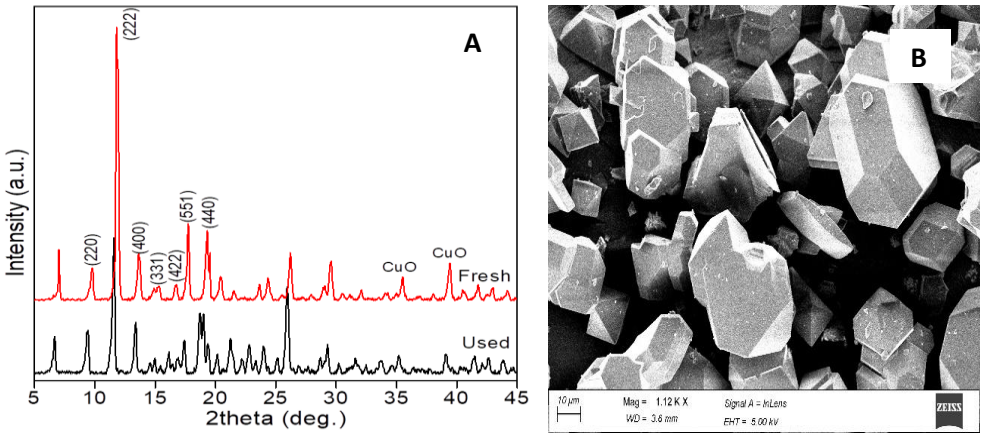

Figure : 11A) Fresh and Used XRD of 0.5S-Cu-Co MOF B) SEM image of used 0.5S-Cu-Co MOF

Table 2: CHNS Analysis of MOF catalysts

Catalyst	Sulphur (%)	Carbon (%)	Hydrogen (%)	Nitrogen (%)
Cu-Co MOF	0	28.56	4.05	3.61
Co MOF	0	29.28	4.13	3.83
0.5S-Cu-Co MOF	6.62	27.53	3.93	1.65
0.5S-Co MOF	5.98	30.27	4.02	3.69
0.5S-Cu-Co MOF (used)	6.32	27.67	3.52	1.58

Glycerol acetalization is reported to follow a Langmuir-Hinshelwood bimolecular first order kinetics [44]. Mechanism is explained to happen in three main steps:

1. Activation of the carbonyl group of acetone over a Lewis/Bronsted acid site either by polarization or protonation [51].
2. Nucleophilic attack of hydroxyl group of glycerol via a carbonium ion to form a hemi-ketal intermediate [52].
3. Elimination of water followed by cyclization resulting in the product formation [50].

The product formed can be a 5-membered dioxolane, solketal which is kinetically favoured product or can be a 6-membered dioxane that is a thermodynamically favoured product. Thus, a higher reaction temperature favours the formation of the later while lower temperature/room temperature reaction results in higher selectivity towards solketal formation [53].

In the present work it seems that both Bronsted as well as Lewis acid sites seem to play role in the reaction mechanism. Initially protonation step probably is initiated by the Bronsted sites but the enhancement of no. of Lewis acid sites is greater than the Bronsted sites with sulphation that suggests the dominant role of Lewis acid sites in defining the selectivity to solketal. The probable mechanism scheme 2 below is proposed to explain the role of both the acid sites available on the surface of sulphated Cu-Co MOF catalyst.

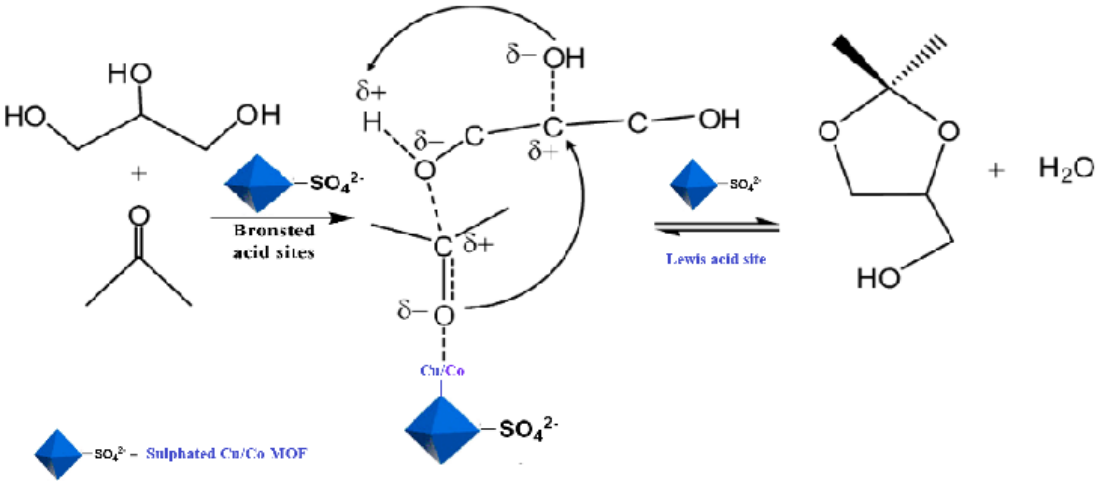

Scheme 2: Probable reaction mechanism of glycerol acetalization over the surface of 0.5S-Cu-Co MOF

IV. Conclusions

A bimetallic Cu-Co MOF was synthesized by solvo thermal technique and modified by sulphation through impregnation method. This catalyst was synthesized to improvise the glycerol acetalization activity for the synthesis of solketal over the Co-MOF that was found to show low conversion of glycerol. Incorporation of Cu in the Co-MOF structure to prepare the bimetallic Cu-Co MOF proved to be beneficial in enhancing the yield of solketal formation. The catalysts in pristine form as well as after sulphation showed intact MOF structure with characteristic diffraction peaks. The MOFs exhibited high specific surface area and also regular cubo octahedral particles that are well defined. The spectroscopic analysis from FT-IR and Raman indicated the characteristic peaks shown by the BTC organic linker along with the vibrational modes of Cu-Cu, Cu-O and Co-O. The sulphated MOFs additionally showed the vibrational modes of sulphate group. The Ex-situ Py-IR clearly indicated the increase in acidity especially Lewis acid sites with incorporation of second metal Cu in the MOF structure and further by sulphation that was attributed to its higher activity as compared to the rest of the MOFs under study. The bimetallic catalyst was studied extensively under variable reaction conditions to optimize the parameters and to obtain maximum activity possible under the ambient conditions. It was found to be stable even after reuse for 5 cycles of reaction run and its structure remaining stable without much loss of sulphate after these 5 times of use in the reaction. The used catalyst XRD, SEM-EDS and CHNS analyses established the stability of the sulphated bimetallic Cu-Co MOF catalyst. Thus, from the above study, sulphated Cu-Co MOF can be suggested as a potential catalyst for the valorization of bio-glycerol to solketal owing to its industrial importance.

Acknowledgements

The authors thank Dr. A. Venugopal, Chief Scientist, C & FC Department, CSIR-IICT, Hyderabad, India for some of the characterization of the catalysts.

References

[1]. Furukawa, H.; Cordova, K.E.; O'Keeffe, M.; Yaghi, O.M. *Science*, **2013**, *341*, 1230444.
[2]. Silva, P.; Vilela, S.M.F.; Tome, J.P.C.; Almeida Paz, F.A. *Chem. Soc. Rev.*, **2015**, *44*, 6774-6803.
[3]. Yap, M.H.; Fow, K.L.; Chen, G.Z. *Green Energy Environ.* **2017**, *2*, 218–245.
[4]. Hsu, S.-H.; Li, C.-T.; Chien, H.-T.; Salunkhe, R.R.; Suzuki, N.; Yamauchi, Y.; Ho, K.-C.; Wu, K.C.W. *Sci. Rep.* **2014**, *4*, 6983.
[5]. Young, C.; Wang, J.; Kim, J.; Sugahara, Y.; Henzie, J.; Yamauchi, Y. *Chem. Mater.* **2018**, *30*, 3379–3386.
[6]. Van Nguyen, C.; Matsagar, B.M.; Yeh, J.-Y.; Chiang, W.-H.; Wu, K.C.W. *Mol. Catal*., **2019**,*475*, 110478.
[7]. Schneemann, A.; Bon, V.; Schwedler, I.; Senkovska, I.; Kaskel,S.; Fischer, R.A. *Chem. Soc. Rev.*, **2014**, *43*, 6062-6096.
[8]. Dhakshinamoorthy, A.; Alvaro, M.; Garcia, H. *Catal. Sci. Technol.,* **2011**, *1*, 856–867.
[9]. Venu, B.; Shirisha, V.; Vishali, B.; Naresh, G.; Kishore, R.; Sreedhar, I.; Venugopal, A. *New J. Chem.*, **2020**,*44*, 5972-5979.
[10]. Zhao, M.; Yuan, K.; Wang, Y.; Li, G.; Guo, J.; Gu, L.; Hu, W.; Zhao, H.; Tang, Z. *Nature*., **2016**, *539,* 76–80.
[11]. Dhakshinamoorthy, A.; Alvaro, M.; Garcia, H. *Adv. Synth. Catal*., **2010**, *352*, 3022–3030.
[12]. Cirujano, F.G.; López-Maya, E.; Rodríguez-Albelo, M.; Barea, E.; Navarro, J.A.; De Vos, D.E. *ChemCatChem* **2017**, *9*, 4019–4023.
[13]. Huang,Y. B.; Liang, J.; Wang, X. S.; Cao, R. *Chem. Soc.Rev.,* **2017**, *46*, 126-157.
[14]. Tian, F.; Qiao, C.; Zheng, R.; Ru, Q.; Sun, X.; Zhang, Y.; Meng, C. *RSC Adv.,* **2019**, *9,* 15642 -15647.

[15]. Kiss, A. A.; Bildea, C. S. *J Chem Technol Biotechnol*., **2012,** *87*, 861–879.
[16]. Tan, H. W.; Aziz, A. R. A.; Aroua, M. K. *Renewable and Sustainable Energy Rev.,* **2013**, *27*, 118–127.
[17]. Kong, P.S.; Aroua, M, K.; Daud, W. M. A. *Renewable and Sustainable Energy Rev*., **2016**, *63*, 533–555.
[18]. Leal-Duaso, A.; Pérez, P.; Mayoral, J.A.; Garciá, J.I.; Pires, E. *ACS Sustainable Chem. Eng*., **2019**, *7*, 13004–130014.
[19]. Leal-Duaso, A.; Pérez, P.; Mayoral, J.A.; Pires, E.; García, J.I. *Phys. Chem. Chem. Phys.,* **2017**, *19*, 28302– 28312.
[20]. Velázquez, D.; Mayoral, J.; García-Peiro, J.; García, J.; Leal-Duaso, A.; Pires, E. *Molecules*., **2018**, *23*, 1–10.
[21]. Monteiroa, M. R.; Kugelmeier, C. L.; Pinheiro, R.S; Batalha, M. O.; Da Silva, C. A. *Renewable and Sustainable Energy Rev*., **2018**, *88*, 109–122.
[22]. Mota, C. J. A.; Da Silva, C. X. A.; Rosenbach, N.; Costa, J.; Da Silva, F. *Energy Fuels*., **2010**, *24*, 2733–2736.
[23]. Rossa, V.; da Pessanha Y, S, P.; Díaz, G. C.; Câmara, L.D.T.; Pergher, S. B. C.; Aranda, D. A. G. *Ind. Eng. Chem. Res*., **2017**, *56*, 479–488.
[24]. Dmitriev, G. S.; Terekhov, A.V.; Zanaveskin, L.N.; Khadzhiev, S.N.; K. L. Zanaveskin, K.L.; Maksimov, A.L. *Russian Journal of Applied Chem*., **2016**, *89*, 1619−1624.
[25]. Gonçalves, M.; Rodrigues, R.; Galhardo, T. S.; Carvalho, W. A. *Fuel*., **2016**, *181*, 46–54.
[26]. Cornejo, A.; Barrio, I.; Campoy, M.; Lázaro, J.; Navarrete, B. *Renewable and Sustainable Energy Rev*., **2017**, *79*, 1400-1413.
[27]. Rodrigues, A.; Bordado, J. C.; Santos, R. G. D. *Energies*., **2017**, *10*, 1817-52.
[28]. Nanda, M. R.; Zhang, Y.; Yuan, Z.; Qin, W.; Ghaziaskar, H. S.; Xu, C. C. *Renewable Sustainable Energy Rev.* **2016**, *56*, 1022−1031.
[29]. Guidi, S.; Noè, M.; Riello, P.; Perosa, A.; Selva, M. *Molecules.* **2016**, *21*, 657.
[30]. Manjunathan, P.; Sanjeev P. M.; Halgeri, A.B.; Ganapati V. S. *Journal of Molecular Catalysis A: Chemical*., **2015,** *396*, 47–54.
[31]. Yadaiah, S.; Venkatesham, K.; Vijayalaxmi, B.; Balakrishna, M.; Sasikumar, B.; Hari Padmasri, A. *IOSR Journal of Applied Chemistry (IOSR-JAC)*., **2023**,*16,* Ser. I ,05-13.
[32]. Balakrishna, M.; Sasikumar, B.; Srinivas, B.; Sarma, A. V. S., Hari Padmasri, A. *Microporous and Mesoporous Materials*., **2024**, *363*, 112830.
[33]. Balakrishna, M.; Sasikumar, B.; Yadaiah, S.; Hari Padmasri, A. *IOSR Journal of Applied Chemistry (IOSR-JAC)*., **2023**, *16*, 01−10.
[34]. Balakrishna, M.; Sasikumar, B.; Srinivas, B.; Sarma, V.S. A.; Hari Padmasri, A. *Energy & Fuels.* **2024**, *38*, 21134-21143.
[35]. Ammaji, S.; Srinivasa Rao, G.; Chary,V.R.K. *Applied Petrochemical Research*., **2018**, *8*, 107–118.
[36]. Bakuru, V.R.; Churipard, S.R.; Maradur, S.P.; Kalidindi, S.B. *Dalton Trans.,* **2019**, *48*, 843–847.
[37]. Jiang, Y.; Zhou, R.; Ye, B.; Hou, Z. *J. Ind. Eng. Chem.,* **2022**, *110*, 357–366.
[38]. Mirante, F.; Leo, P.; Dias, C .N.; Cunha-Silva, L.; Balula, S.S. *Materials*., **2023**, *16*, 7023.
[39]. Chen, Y.; Mu, X.; Lester, E.; Wu, T. *Prog. Nat. Sci. Mater. Int*., **2018**, *28*, 584–589.
[40]. Abrori, S. A.; Trisno, M. L. A.; Aritonang, R. A.; Anshori, I.; Nugraha,; Suyatman,; Yuliarto, B. *IOP Conf. Ser.: Mater. Sci. Eng.,* **2021**, *1045*, 012006.
[41]. Gharagozlou, M.; Eskandari, K.; Sadjad, S.; *J. Mater. Sci.: Mater. Electron.,* **2023,** *34*, 778.
[42]. Arjamand, F.; Ranjbar, Z. R.; *Scientific Reports*., **2024**, *14(1)*, 12843.
[43]. Wagh, K. V.; Gajengi, A. L.; Rath, D.; Parida, K. M.; Bhanage, B. M. *Mol. Catalysis*., **2018**, *452*, 46-53.
[44]. Selvaraj, M.; Pandurangan, A.; Seshadri, K.; Sinha, P.; Krishnasamy, V.; Lal, K. B. *J. Mol. Cat. A. Chemical*., ***2003****, 192,* 153-170.
[45]. Dybtsev, D.N.; Yutkin, M.P.; Peresypkina E.V.; Virovets A.V.; Hasegawa Y.; Nishihara, H.; Fedin, V.P.; *Russ. Chem. Bull.***, 2007**, *56,* 1782–1786.
[46]. Arul, P.; Gowthaman, N.S.K.; John, S.A.; Tominaga, M. *Electrochim. Acta***., 2020,** *354,* 136673.
[47]. Dong, Z.; Mi, Z.; Shi, W.; Jiang, H.; Zheng, Y.; Yang, K. *RSC Adv.* **2017,** *7,* 55504–55512.
[48]. Deutsch, J.; Martin, A.; Lieske, H. *J. Catal.,* **2007**, *245*, 428–435.
[49]. Carolina, X. A. D.; Valter, L. C. G.; Claudio, J. A. M. *Green Chem*., **2009**,*11*, 38-41
[50]. Li, Li.; Tamás, I. K.; Bert, F.S.; Paolo P. P. *Green Chem*., **2012***, 14*, 1611-1619
[51]. Menezes, F D. L.; Guimaraes, M D. O.; da Silva, M. J. *Ind. Eng. Chem. Res.,* **2013,** *52*, 16709−16713.
[52]. Talebian-Kiakalaieh, A.; Tarighi, S. *J. Ind. Eng. Chem.,* **2019,** *79*, 452–464.
[53]. Wegenhart, B. L.; Liu, S.; Thom, M.; Stanley, D.; Abu-Omar, M.M. *ACS Catal.,* **2012,** *2,* 2524.